ORIGINAL PAPER

A comparative study of analytic representations of potential energy curves for O_2, N_2, and SO in their ground electronic states

Judith P. Araújo[1] · Marcos D. Alves[1] · Ramon S. da Silva[1] · Maikel Y. Ballester[1]

Abstract

In this work, a review of six functional forms used to represent potential energy curves (PECs) is presented. The starting point is the Rydberg potential, followed by functions by Hulburt–Hirschfelder, Murrell–Sorbie, Thakkar, Hua and finalizing with the potential for diatomic systems by Aguado and Paniagua. The mathematical behavior of these functions for the short- and long-range regions is discussed. A comparison highlighting the positive and negative aspects of each representation is also presented. As study cases, three diatomic systems O_2, N_2 and SO in their respective ground electronic states were selected. To obtain spectroscopic parameters, *ab initio* energies were first calculated at multi-reference configuration interaction (MRCI) with the Davidson modification (MRCI+Q) level of theory, using aug-cc-pVXZ (X = T,Q,5,6) Dunning basis sets. Such energies were then fitted to respective functional forms. The so-obtained spectroscopic constants are compared also with available literature data.

Keywords Potential energy curves · Diatomic systems · Spectroscopic parameters · *ab initio* calculations

Introduction

The relationship between the potential energy and the internuclear distance of two atoms is of the greatest importance in physical chemistry. The study of processes like molecular scattering, photodissociation, chemical kinetics, and electric discharges relies on the knowledge of these functions [1–6]. Due to practical limitations in the solution of the Schrödinger equation for a molecular system, physically supported approximations are required. In 1927, Born and Oppenheimer, also with the contribution of Huang, presented a pathway to circumvent this problem [7].

✉ Judith P. Araújo
judith.araujo@ifsudestemg.edu.br

Maikel Y. Ballester
maikel.ballester@ufjf.edu.br

1   Departamento de Física, Universidade Federal de Juiz de Fora, Juiz de Fora, MG Brazil

The Born–Oppenheimer approximation (BOA) consists of the separation of the nuclear and electron motions: once nuclei have much larger masses than the electron (more than 1838 times), they can be considered as stationary compared to the moving electrons. The mathematical formalism for such an approach can be followed elsewhere [7] and is fundamental in understanding the key concept of potential energy surface (PES). Within BOA, nuclei in a molecular system move on the PES resulting from the solution of the electronic problem. Since BOA, several researchers have been attempting to obtain analytic representations of energy as a function of the interatomic distances. Such a representation is usually required to be mathematically simple while accurately reproducing theoretical and experimental data.

The potential energy curve provides broad insight into the structure of a molecular system. The minimum in this curve defines the bond length of the diatomic molecule. Its second derivative provides the force constants, from which vibrational and rotational energy levels of the molecule can be calculated. Higher-order derivatives are required for the calculation of the anharmonicity constants.

Among the analytical representations available in the literature (over 50 to our knowledge), six functions were chosen: Rydberg, Hulburt–Hirschfelder, Murrell–Sorbie, Thakkar, Hua, and Aguado-Camacho-Paniagua.

This selection was motivated considering that the first three were proposed a long time ago, and the curves were obtained theoretically or semi-empirically, in the case in which the functions were based on a compromise between results of empirical measures of experimental character and few reliable theoretical calculations available until the mid-1980s, except for very simple diatomic systems [8]. In counterpart, the latter three potentials Thakkar, Hua, and Aguado-Paniagua, had been presented using *ab initio* calculations together with semi-empirical calculation techniques. Thus, the aim of this work is to apply *ab initio* calculation techniques to the earliest potentials and compare them with more recent ones using O_2, N_2, and SO as case study diatomic systems.

This paper is organized as follows. Section "Potential curves" contains a wide description of the interest PECs. A discussion about technical details for theoretical calculations is presented in "Electronic structure calculations". The results are gathered in "Results and discussion" and the conclusions are given in the last section.

Potential energy curves

The Rydberg function

The potential functions used before Rydberg proposal described only the lowest vibrational levels and were not useful in the extrapolation to dissociation limit [9]. It was then necessary to seek more general analytical ways to describe potential energy functions for diatomic systems, best fitting also the dissociation region. Moreover, an accurate representation of the series of nuclear vibrations was not known, and nuclear vibrations are experimentally measured in terms of ΔG, being $\Delta G = G(v + 1) - G(v)$, where $G(v)$ is the nuclear vibrational energy corresponding to the quantum number v. Then ΔG is assumed to be a linear function of the quantum number v, approximation valid only for the simple diatomic system H_2. For somewhat more complex systems like N_2, O_2 and NO, a function of the type $(\Delta G)^2$ was used, more properly describing the nuclear vibrations. However, such a function still depended only on the quantum number v. It was then, in 1931, when Rydberg [9] suggested an empirical relationship between $(\Delta G)^2$ and B_v:

$$(\Delta G)_v^2 = f \cdot B_{v+1}^3 \tag{1}$$

where

$$B_v = \frac{\hbar}{8\pi^2} \left(\overline{\frac{1}{\mu R^2}} \right)_v, \tag{2}$$

is the rotational constants, f is the force constant, and μ is the reduced mass.

The relation in Eq. 1 depends entirely on the behavior of the potential curve, i.e., the forces acting on the atomic nuclei. Rydberg showed the potential V(R) for H_2, CdH and O_2 required further fine-tuning to meet the conditions of Oldenberg and Hulthén [9]:

1. $\oint pdR = \oint [2\mu(V(R)-E_v)]^{\frac{1}{2}} dR = \hbar \left(v + \frac{1}{2} \right)$

2. $\left(\frac{1}{R^2} \right)_v = \frac{\omega_v \cdot \sqrt{\mu}}{\sqrt{2}} \oint \frac{dR}{R^2 \sqrt{V(R)-E_v}}.$

Seeking a potential simultaneously fulfilling both conditions, Rydberg [9] proposed the following potential function:

$$V_{Ryd} = -D_e(a(R-R_e) + 1)e^{-a(R-R_e)} \tag{3}$$

where $a = (f/D_e)^{\frac{1}{2}}$, being f give by $f = \left(\frac{d^2 V_R}{dR^2} \right)_{R_e}$. Here, D_e should not be confused with the dissociation energy D, since $D_e - D = \frac{1}{2}\hbar\omega_e$. In this equation, f represents the force constant. V_R becomes large, but not infinite when R = 0, similarly than Morse potential [10]. However, Rydberg showed that its potential provided best fitting compared to Morse function for the three diatomic systems mentioned before H_2, CdH and O_2.

From the third- and fourth-order derivatives of $V_R(R_e)$ it is possible to obtain the values for the spectroscopic parameters α and $\omega_e x_e$ as shown by Varshni [11]:

$$\alpha = \left[\frac{2\sqrt{2}}{3} \left(\frac{f R_e^2}{2D_e} \right)^{\frac{1}{2}} - 1 \right] \frac{6B_e}{\omega_e} \tag{4}$$

and

$$\omega_e x_e = \frac{22}{3} \left(\frac{f R_e^2}{2D_e} \right) \cdot \frac{2.1078 \times 10^{-16}}{R_e^2 \mu} \tag{5}$$

where $B_e = \hbar/(8\pi^2 \mu R_e c)$.

The Hulburt–Hirschfelder function

The Morse [10] function was considered limited due to the reduced number of parameters, initially seen as an advantage. To tackle this limitation, in 1940, Hulburt and Hirschfelder [12] suggested the addition of two parameters, i.e., functions involving five spectroscopic constants. These two parameters to be added in a so-called correction term were easily determined, and the five-parameter functions proved satisfactory for a large majority of diatomic molecules. However, the problem to obtain the potential V(R) already reported in the Morse function for large internuclear distances was not solved with this correction. Since the high levels of vibrational energy are unknown for many molecules, it is virtually impossible to find a

unique potential that could be universally used for diatomic systems.

From the fact that the spectroscopic constants ω_e, $\omega_e x_e$, $B_e = \hbar/(8\pi^2 \mu R_e c)$ and α are known for most diatomic molecules, the function proposed by them, used three parameters to recover the usual Morse function [10] plus two parameters, b and c, correcting Morse potential, and at the same time were obtained by means of the known constants. The function of Hulburt and Hirschfelder, here called the HH potential, has the form:

$$V_{HH} = D_e[(1 - e^{-x})^2 + (1 + bx)cx^3 e^{-2x}] \quad (6)$$

where $x = \dfrac{\omega_e}{2(B_e D_e)^{\frac{1}{2}}} \left[\dfrac{R\text{-}R_e}{R_e}\right]$, and the constants b and c are:

$$c = 1 + a_1 (D_e/a_0)^{\frac{1}{2}}, \quad (7)$$

$$b = 2 + \dfrac{\left[\dfrac{7}{12} - \dfrac{D_e a_2}{a_0}\right]}{c} \quad (8)$$

being a_0, a_1 and a_2 the Dunham coefficients given by expansion [13]

$$a_0 = \omega_e^2/4B_e \quad (9)$$

$$a_1 = -1 - \alpha \omega_e/6B_e^2 \quad (10)$$

$$a_2 = \dfrac{5}{4}a_1^2 - \dfrac{2}{3}\dfrac{\omega_e x_e}{B_e}. \quad (11)$$

To represent the potential HH (6) as a function of the nuclear distance R, x is rewritten as $x = \beta(R - R_e)$, where

$$\beta = \dfrac{\omega_e}{2R_e(B_e D_e)^{\frac{1}{2}}} \quad (12)$$

thus, V_{HH} becomes:

$$V_{HH} = D_e[(1 - e^{-\beta(R-R_e)})^2$$
$$+(1 + b\beta(R - R_e))c\beta^3(R - R_e)^3 e^{-2\beta(R-R_e)}] \quad (13)$$

The potential of HH was introduced aiming at better fit spectroscopic constants. Nevertheless, it is difficult to find a suitable polynomial to express both the lowest and the highest vibrational energy levels. For this goal, the polynomial function was then multiplied by an exponential term:

$$E_v = A[1 - \exp(-1/2(v + 1/2))]$$
$$\times \left[1 + 0,1\left(v + \dfrac{1}{2}\right) - 0.005\left(v + \dfrac{1}{2}\right)^2\right]. \quad (14)$$

The energy levels, for small values of $(v + 1/2)$, are calculated by the series [12]:

$$E_v/\text{kcal mol}^{-1} = 0,5\left(v + \dfrac{1}{2}\right) - 0.075\left(v + \dfrac{1}{2}\right)^2 + \cdots, \quad (15)$$

while for corresponding high values the following series is used:

$$E_v/\text{kcal mol}^{-1} = 1 + 0,1\left(v + \dfrac{1}{2}\right) - 0.005\left(v + \dfrac{1}{2}\right)^2 + \cdots. \quad (16)$$

The method to obtain the corresponding energy levels would replace (13) in the Schrödinger equation and perform numerical integrations.

In 1961, Hulburt and Hirschfelder [14] perceived an error in the first sign of the expression for the parameter b, the corrected signal is negative not positive, i.e.,

$$b = 2 - \dfrac{\left[\dfrac{7}{12} - \dfrac{D_e a_2}{a_0}\right]}{c}. \quad (17)$$

This led researchers as Tawde [15] and Herzberg [16] to question the fit of their potential function, being considered poorly fitted because of this error. In a paper published in 1954, Tawde and Gopalakrishnan [15] even stated that the fitting of the HH function was good only for distances larger than the equilibrium distance, i.e., for R¿R$_e$ in the case of the C$_2$ molecule. However, after analyzing the potential with the correct sign in parameter b, Tawde and Katti, who were the first to notice and communicate the authors about the error in b, concluded that the function by Hulburt and Hirschfelder was indeed a good representation [17].

The Murrell and Sorbie function

In 1974, the Morse [10] potential was still considered one of the most popular to describe the PES of diatomic systems. The potential of Hulburt and Hirschfelder [12] was also well known for improving Morse potential, as it corrected the long region of the function. Furthermore, the Rydberg [9] potential, largely used by spectroscopists, with its simple functional form, differing little from the potential of Morse, was also a reference at the time to describe such systems.

Taking these three potentials into consideration, seeking for a functional shape best representing various diatomic systems, Murrell and Sorbie [18] proposed a modification of the Rydberg [9] function. They then compared this new potential with results obtained using Morse [10] and Hulburt-Hirschfelder [12] functions, taking as reference the fitting obtained by the RKR method [9, 19, 20].

The original potential function by Rydberg [9] is:

$$V_R = -D_e[1 + a(R\text{-}R_e)]\exp(-a(R\text{-}R_e)) \quad (18)$$

where D_e is the well depth

$$a = (f/D_e)^{1/2} \tag{19}$$

being the n order derivatives given by:

$$f^{(n)} = f(-1)^n(n-1)a^{(n-2)} \tag{20}$$

where f is the force constant.

   MS began to investigate the properties of the modified potentials of Rydberg [9],

$$V = \left(-D_e \frac{\left[\sum_n a_n(R-R_e)^n\right]}{\sum_m b_m(R-R_e)^m}\right)e^{-\gamma(R-R_e)}. \tag{21}$$

For the calculation of a_n and b_n in Eq. 21, MS assumed $a_0 = b_0 = 1$, while spectroscopic expansion was used for other parameters:

$$V = -D_e + \frac{1}{2}\sum_{n=2}F_n(R-R_e)^n = -D_e\sum_{n=0}G_n(R-R_e)^n;$$
$$F_n = 2f^{(n)}/n!,$$
$$G_n = -F_n/2D_e \text{ and } G_0 = 1, \; G_1 = 0 \tag{22}$$

or more conveniently

$$a_n = \sum_{s=0}^{n}G_{n-s}\sum_{t=0}^{s}b_t\gamma^{s-t}/(s-t)!. \tag{23}$$

Since $F_1 = [2\,(dV/dR)_{R_e}]/n! = 0$, and the spectroscopic parameters F_2, F_3 and F_4 are known, MS [18] imposed three conditions warrantying the solutions of Eq. 23 are physically acceptable. These are:

1. γ shall be positive;
2. There shall be no zeros of the b-polynomial in the region physically significant R (i.e., all positive and small negative R);
3. There shall be no maxima in the attractive branch of the potential.

   Murrell and Sorbie analyzed all cases of potential (21) having the following sets of non-zero coefficients: (a_1, a_2, a_3); (a_1, a_2, b_1); (a_1, a_3, a_4); (a_1, a_3, a_1); (a_1, a_1, a_2); and (b_1, b_2, b_3). The only combination leading to a satisfactory potential to describe the long-range region was the first one. The potential (21) then takes the form:

$$V_{MS} = D_e(1+a_1(R-R_e)+a_2(R-R_e)^2+a_3(R-R_e)^3)e^{-\gamma(R-R_e)} \tag{24}$$

where the constants a_1, a_2 and a_3 and γ are obtained through the coupled relations:

$$a_1 = \gamma$$
$$a_2 = G_2 + \gamma^2/2$$
$$a_3 = G_3 + \gamma G_2 + \gamma^3/6$$
$$0 = G_4 + \gamma G_3 + \gamma^2 G_2/2 + \gamma^4/24 \tag{25}$$

The last equation in Eq. 25 has at least one positive root, as condition 1 demands. Its solution is numerically obtained.

The Thakkar function

In 1975, Thakkar [21] proposed a new and generalized power series expansion for diatomic potentials. There, a nonlinear parameter *p*, leading to both Dunham [13] and SPF [22] expansions as special cases were used. The function assumed the form:

$$V_T(R) = e_0(p)\lambda^2\left[1 + \sum_{n=1}^{\infty}e_n(p)\lambda^n\right] \tag{26}$$

where

$$\lambda(R,p) = s(p)[1 - (R_e - R)^p] \tag{27}$$

being p a nonzero number, R_e the equilibrium internuclear separation and s(p) an abbreviated notation for the *sgn* function defined for

$$s(p) = \text{sgn}(p) = \begin{cases} +1, & p > 0 \\ -1, & p < 0 \end{cases}. \tag{28}$$

For $p = -1$, the Eq. 26 becomes

$$V(R) = a_0[R-R_e/R_e]^2\left\{1 + \sum_{n=1}^{\infty}a_n[R-R_e/R_e]^n\right\} \tag{29}$$

where $a_n = e_n(-1)$, and the Eq. 29 is exactly the Dunham expansion [13].

   For $p = +1$, the Eq. 26 becomes

$$V(R) = b_0[R-R_e/R]^2\left\{1 + \sum_{n=1}^{\infty}b_n[R-R_e/R]^n\right\} \tag{30}$$

where $b_n = e_n(1)$, and the Eq. 30 is exactly the SPF expansion [22].

   Still, for $p > 0$ and $e_n(p) = 0(p \geq 1)$ the Eq. 26 becomes:

$$V(R) = e_0(p) + e_0(p)[(R_e/R)^{2p} - 2(R_e/R)^p] \tag{31}$$

which is simply the Leonard–Jones (2p, p) potential [23].

   The radius of convergence of the Eq. 26 is determined by the singularity of $V_T(R)$ closest to $R = R_e$ in the complex R plane. For $p < 0$, the singularity occurs at $(R^{|p|} - R_e^{|p|})/R_e^{|p|} = -1$, which implies that for $p < 0$ the potential (26) cannot converge for $R > 2^{1/|p|}R_e$ [21]. In the case of Dunham potential ($p = -1$), as pointed out in SPF [22], the expansion can not converge to $R > R_e$. For $p > 0$, the pole at $R = 0$ occurs at $(R^p - R_e^p)/R^p = -\infty$, and therefore the radius of convergence of Eq. 26 is limited by infinity.

   Thakkar [21] conjectured that the Eq. 26 converges to R in the interval $(0, 2^{1/|p|}R_e)$ for $p < 0$ and converges to R in the interval $(0, \infty)$ for $p > 0$, converging faster only in the interval $(R_e/2^{1/|p|}, \infty)$ for $p > 0$. For the calculation

of the coefficients $e_n(p)$ in the expansion (26), Thakkar adapted the Dunham [13] procedure, and obtained a relation between $e_n(p)$ and a_n [21].

Regarding the choice of p, $p > 0$ values produce better results since the potential converges rapidly in the long-range region, which is of great interest for molecular dynamics studies. Thakkar [21], proposes

$$p = -a_1 - 1 \qquad (32)$$

and estimates some values for p through the extensive Calder and Reudenberg analysis of the Dunham coefficients for 160 diatomic molecules [21].

Thakkar analyzed the behavior of the potential $V_T(R)$, with p given by the relation (32) using the truncated expansion:

$$V_T^N(R) = e_0(p)\lambda^2 \left[1 + \sum_{n=1}^{N} e_n(p)\lambda^n \right]. \qquad (33)$$

The dissociation energy D is given by:

$$D^N = e_0(p) \left[1 + \sum_{n=1}^{N} e_n(p) \right], \; p > 0 \qquad (34)$$

being p calculated by Eq. 32.

The Hua function

In 1990, Hua [24] conducted a comparative study with the potentials of Morse [10], Varshni [11] and Levine [25]. These three potentials had a common characteristic: all showed large deviations compared to RKR curves [9, 19, 20] when the domain of the potential is extended to the limit of dissociation. Moreover, for the potentials of Varshni and Levine the Schrödinger equation can be exactly solved, with rather complicate calculations [24].

With this in mind, in order to meet both requirements, Hua proposes a potential of four parameters, which is accurate in the dissociation limit and exactly solve the Schrödinger equation in a simpler manner. Such a function is given by:

$$V_H(R) = D_e \left[\frac{1 - e^{-b(R-R_e)}}{1 - c e^{-b(R-R_e)}} \right]^2, \; |c| < 1 \qquad (35)$$

with

$$b = \alpha(1-c) \qquad (36)$$

being α the same of the Morse function [10]. The parameter c is fitted as to minimize mean deviations.

The function of Hua V_H has the advantage that when inserted into the Schrödinger equation, it can be solved exactly for angular momentum $J = 0$ and can be treated precisely for $J \neq 0$, allowing to calculate the corresponding ro-vibrational energy levels for a given system.

The four parameters potential of Hua gained prominence because it presented a good fit for the systems tested [24] in the total potential, both in the spectroscopic region and in the dissociation limit. Such results were obtained even for large domains, dispensing a piece-wise fitting of the potential without requiring spline functions associated or other functions, as is the case of the Morse potential (see for example [27]).

The Aguado and Paniagua function

One of the simplest and generally successful methods of obtaining potential energy curves for diatomic systems directly from spectroscopic data is through the RKR methods [9, 19, 20], as already mentioned in previous sections. Such methodology is also used in comparisons to verify the quality of the fitted potential. However, the results obtained by the RKR method are presented in the form of tables containing, in general, the numbers ν, $G(\nu)$, B_ν, R_+ and R_-, not being very convenient for a rapid interpretation of the potential behavior.

Aiming at producing accurate and well-behaved potential energy curves in 1992, Aguado, Camacho and Paniagua [1] (ACP) presented a simple functional form, similar to the perturbed-Morse-oscillator (PMO) potential, with better results mainly for the long-range region.

For a tabulated function $y_i = f(x_i)$ $(i = 1, 2, \cdots, n)$, where y_i are the observed $G(\nu) + Y_{00}$ and x_i are the turning points rotation potential curve, ACP suggested a approximated potential function V_{ACP} written as a linear combination of functions ϕ that will be conveniently chosen,

$$V_{ACP} = \sum_{k=0}^{m} c_k \phi_k(x) \qquad (37)$$

where $\phi_k(x)$ belongs to the basis of functions $\{\phi_k\}$, $k = 0, 1, \cdots, m$.

To calculate error vector Q, with components q_i given by $q_i = V(x_i) - y_i$, related RKR data, the method the maximum norm that uses the Chebyshev technique was chosen. Such a methodology was selected because of the interest in getting an error vector Q with a limited value point by point [1]. Within this method, the problem is to find the $c_0, c_1, \cdots c_m$ parameters of the Eq. 37.

The chosen basis function was one that contains functions similar to PMO

$$\phi_k(x) = [1 - e^{\beta x}]^k, \; k = 0, 1, \cdots, m. \qquad (38)$$

where β is a nonlinear parameter independently set to obtain the best approximation and $x = R - R_e$, with R and R_e as already defined in this work.

The procedure proposed by ACP [1] to obtain the energies and consequently of the potential energy curves for

the systems of interest, starts with the use of V_{ACP} (37) and the functions ϕ_k (38) in the radial equation of Schrödinger for $J = 0$:

$$\left(-\frac{\hbar}{4\pi\mu c}\frac{d^2}{dR^2} + V(R)\right)\psi_\nu = E_\nu\psi_\nu \qquad (39)$$

Its resolution is carried out through the diagonalization of the Hamiltonian matrix, in order to obtain the eigenvalues E_ν. For this, Hermite functions are used as orthogonal basis set:

$$\chi_n(x) = e^{-\alpha x^2/2}H_n(\alpha^{1/2}x), \quad n = 0, 1, 2\cdots \qquad (40)$$

where H_n are the Hermite polynomials and $\alpha \approx 2\pi\nu_e\mu/\hbar$.

The Hamiltonian matrix is obtained through of the integrals $V_{nm} = <\chi_n|e^{-\beta jx}|\chi_m>$, which can be calculated using the recurrence relation,

$$V_{nm} = -\frac{\beta j}{\alpha^{1/2}}V_{n-1m} + 2mV_{n-1m-1} \qquad (41)$$

where the first column $(m = 0)$, provides $V_{00} = \left(\frac{\pi}{\alpha}\right)^{1/2} e^{\frac{\beta^2 j^2}{4\alpha}}$.

In 1992, Aguado and Paniagua [26] proposed a functional form to obtain analytical potentials of triatomic molecules ABC, in which the full potential was written as an many-body-expansion (MBE) [27]:

$$V_{ABC} = \sum_A V_A^{(1)} + V_{AB}^{(2)}(R_{AB}) + V_{ABC}^{(3)}(R_{AB}, R_{AC}, R_{BC}) \qquad (42)$$

where R_{AB}, R_{AC} and R_{BC} are the internuclear distances and the sums are over all the terms of a given type and where $V_A^{(1)}$ is the energy of atom A in its appropriate electronic state; $V_{AB}^{(2)}$ is the two-body energy that corresponds to the diatomic potential energy curve which vanishes asymptotically when $R_{AB} \rightarrow \infty$ and goes to infinity when $R_{AB} \rightarrow 0$; $V_{ABC}^{(3)}$ is the three-body energy.

As the two-body terms represent the potential energy curve for a diatomic molecule, the functional form selected for the fit must depends on the general behavior of such potential curve. The diatomic terms $V_{AB}^{(2)}$ of the potential (42) are expressed as a sum of two terms corresponding to the short- and long-range potentials, and will be called V_{AP} [26]:

$$V_{AP}^{(2)} = V_{short}^{(2)} + V_{long}^{(2)} \qquad (43)$$

where

$$V_{short}^{(2)} = \frac{c_0 e^{-\alpha_{AB}R_{AB}}}{R_{AB}} \qquad (44)$$

and

$$V_{long}^{(2)} = \sum_{i=1}^{N} c_i \rho_{AB}^i \qquad (45)$$

where (44), with the restriction $c_0 > 0$, ensures that the diatomic potential goes to infinity when $R_{AB} \rightarrow 0$. Aguado and Paniagua [28] showed that a modified form of the functions, introduced by Rydberg [9], in the polynomial variables ρ, given by Eq. 43

$$\rho_{AB} = R_{AB}e^{-\beta_{AB}^{(2)}R_{AB}}, \quad \beta_{AB}^{(2)} > 0 \qquad (46)$$

The linear parameters c_i, $i = 0, 1, ..., N$ and the nonlinear parameters α_{AB}, both in the Eq. 43 and β_{AB} (46) are determined by fitting the *ab initio* energies for the diatomic fragments computed at the same level of theory than the used in the triatomic system [26].

Although it is a proposition for a triatomic potential, the two-body term V_{AP} in Eq. 43 was known as a new diatomic potential of Aguado and Paniagua, being very used today due to its high precision for several systems, in excited states including (see for example Ref. [29]).

Electronic structure calculations

In order to obtain a sufficiently accurate potential energy curve, the electronic structure calculations for the homo-and heteronuclear systems were carried out using as reference complete active space self-consistent (CASSCF) [30] wave function. Dynamical correlation effects were included by means internally contracted multi-reference configuration interaction (MRCI) [31]. Such a strategy has been previously applied in several diatomic molecules [32–34]. Furthermore, the multi-reference Davidson correction (+Q) was included to compensate for the effects of higher-order correlation. The aug-cc-pVXZ (X = T,Q,5,6) basis sets of Dunning were employed. For each basis set, we have performed CASSCF followed by MRCI approach. It must be also highlighted that for the sulfur atom, we have used the Dunning correlation consistent basis set (aug-cc-pV(X+d)Z), which contain an additional d function for the purpose of partially ameliorating a known SCF-level deficiency in the AVXZ sets for second-row elements of periodic table [35].

All calculations were performed with the Molpro 2012 package of *ab initio* programs [36]. We must point out that Molpro only uses Abelian point group symmetry. Following this, we consider irreducible representations of the $D_{\infty h}$ point group for homonuclear molecules (N_2 and O_2) but due to limitations of the procedure, we adopted D_{2h} subgroup of $D_{\infty h}$ point group in the calculations; for SO, C_{2v} subgroup of $C_{\infty v}$ is used. In general, the mapping calculations of the PEC were made at intervals of 0.025 a_0 over the internuclear distance range from 1.0 to 15.0 a_0, where a_0 is the Bohr radius.

Results and discussion

Performance analysis

We start this discussion showing the results obtained from the root-mean-square deviation (RMSD) for the different potentials, basis set and diatomic systems. From the statistical point of view, RMSD values are generally used to evaluate the error of the PEC in relation to the curve obtained via the points *ab initio* data. The root-mean-square deviation is calculated by:

$$\Delta E_{RMSD} = \left[\frac{1}{N} \sum_{i=1}^{N} (V_{ab\ initio} - V)^2 \right]^{1/2} \qquad (47)$$

where $V_{ab\ initio}$ represents the *ab initio* points and V is the potential energy given by four analytic forms selected among those previously presented.

To obtain the two-body energies, we have employed the functions of Rydberg (RYD), Murrell and Sorbie (MS), Hulburt–Hirschfelder (HH), and Aguado and Paniagua (AP). These potentials are very well documented in the literature being, accordingly, good models for this study [37–39]. We remember, of course, that the smaller RMSD values represents the better performance of the fit. To avoid long tables of coefficients, only the results calculated using these functions set are shown. The remaining data are gathered in the Supplementary Materials.

To investigate in details the quality of the fits, graphics of the calculated RMSD values for N_2, O_2, and SO molecules can be seen in Fig. 1. As expected, the best results are found when the AP function is used in combination with a higher basis set, so that for the three systems, differences in the order of 0.10, 0.04, and 0.02 kcal/mol were obtained from other data, respectively.

The ability of the other analyzed potentials, Ryd, MS, and HH, to reproduce *ab initio* points [calculated mainly in the intermediate region] can be clearly seen in the Fig. 2. The Ryd function is represented by a red solid line, while MS is in blue. In black are shown the results of the HH functions and those for AP are in magenta.

Comparing the RMSD test, in almost all cases the fits are above the threshold of chemical accuracy (1 kcal/mol) [40]. In particular, the AP function shows good performance with RMSD values below 0.25 kcal/mol. For sulfur monoxide Fig. 1c, note the very poor quality and the greater deviation of the fit in the AV(T+d)Z when the MS function is applied (RMSD value close to 7 kcal/mol). In such a figure, the values of ΔE_{RMSD} for Rydberg function (2.75, 3.04, 3.21, 3.07 kcal/mol) are not significantly modified when changing the basis set. The same behavior is observed for the MS potential (1.41, 1.42, 1.37 kcal/mol) in the basis sets AV(X+d)Z (X = Q,5,6).

In the case of nitrogen molecule (Fig. 1a), when the Ryd potential is applied, unexpectedly the values of ΔE_{RMSD} increases monotonically as the basis sets increases from AVTZ (2.16 kcal/mol) to AV6Z (2.77 kcal/mol). For the Hulburt–Hirschfelder function, the average value of the RMSD is around 2.0 kcal/mol. For the MS function, although 0.55 kcal/mol be the smaller value of RMSD found at AVQZ, the other basis sets present bigger values, near to 1.80 kcal/mol. The Aguado and Paniagua potential led to deviations of the magnitude of 0.10 kcal/mol these values being close to those found by Xiao-Niu et al. (0.09 kcal/mol) [41].

Finally, the plot of the oxygen molecule represented in Fig. 1b demonstrated a Gaussian-like behavior for the Ryd, MS, and HH functions with a peak at 2.80, 1.25, and 2.50 kcal/mol, respectively. Again, the lower RMSD values are found for the potential AP with a value of approximately 0.04 kcal/mol. As can be noted, the quality of the computed potentials critically depends upon the size of the basis set employed.

To conclude this section, the potential energy curves for ground electronic states of N_2, O_2, and SO, are plotted in Figs. 3, 4 and 5. For convenience, in both cases, we used only the analytical representation proposed by Aguado and Paniagua (see Eq. 43) together with basis set aug-cc-pVXZ where X is the cardinal number of the basis set (X = T, Q, 5, 6). For comparison, the theoretical data are available in Refs. [42] for N_2, [44] for O_2, and [45, 46] for SO are also included in this work. We justify the choice of these works mainly because their results reproduce well the experimental energies. Therefore, they are very close to spectroscopic accuracy.

Figure 3 exhibits the curves for the ground electronic state of the N_2 molecule obtained in this work, along with the PEC extracted from the double many-body expansion (DMBE) potential energy surface for ground state HN_2 [42]. We highlight that the analytical form used by Poveda and Varandas to fit the *ab initio* points for nitrogen molecule is based on the EHFACE2U model [43]. It can be seen from this plot that the potential curves computed for AV5Z (dashed black line) and AV6Z (dashed magenta line) indicate excellent agreement for all points except in the region between $3.5 \leq R/a_0 \leq 5.0$, where the energies of the EHFACE model (circles) are lower than our potential curves. In addition, the major difference (around of 0.013 E_h or 0.35 eV) is observed in the zoom of this same figure if we compare the energies calculated at AVTZ (solid red line) basis set and the EHFACE model in the range of 1.8 a_0 to 2.4 a_0.

Figure 4 shows our potential energy curves now for the oxygen molecule, together with the *ab initio* energies reported by Bytautas et al. [44]. The electronic energies
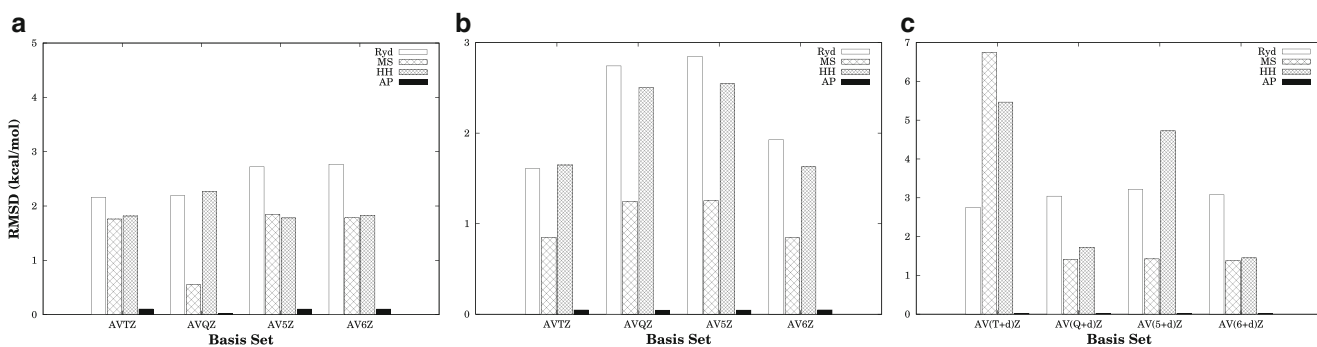
Fig. 1 Root-mean-squared deviation of diatomic molecules: **a** $N_2(X^1\Sigma_g^+)$, **b** $O_2(X^3\Sigma_g^-)$, **c** $SO(X^3\Sigma^-)$ calculated in different basis set and potentials

Fig. 2 Potential energy curves for N_2, O_2, and SO calculated at the MRCI+Q/AV6Z level of theory

Fig. 3 Potential energy curves for the ground electronic state of the N_2 molecule calculated with different basis sets. The *circles* represent energies calculated by EHFACE model from Ref. [42]. In addition, also plotted in the inset is a zoom of the minimum region of the curve
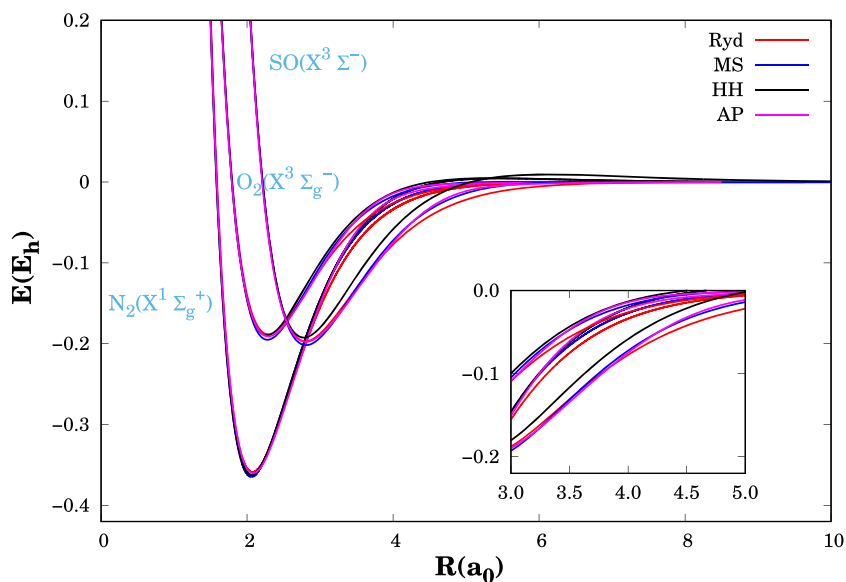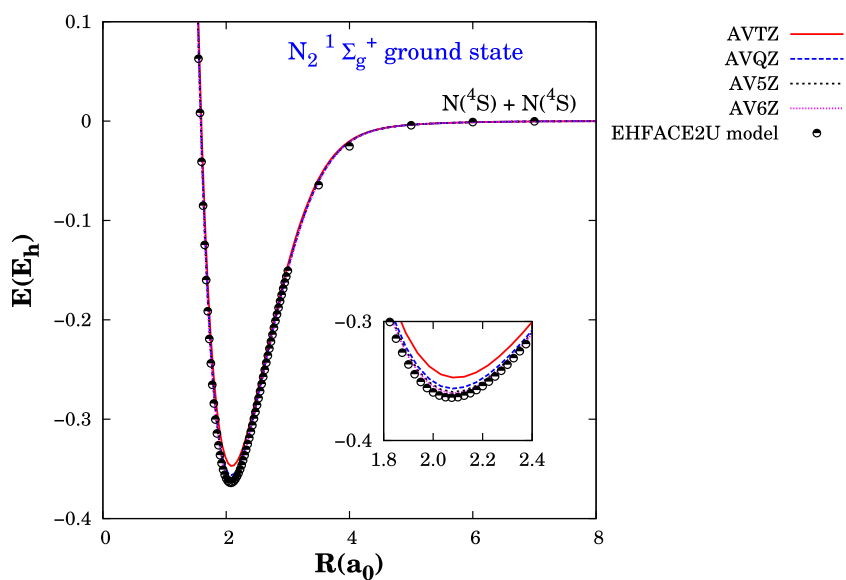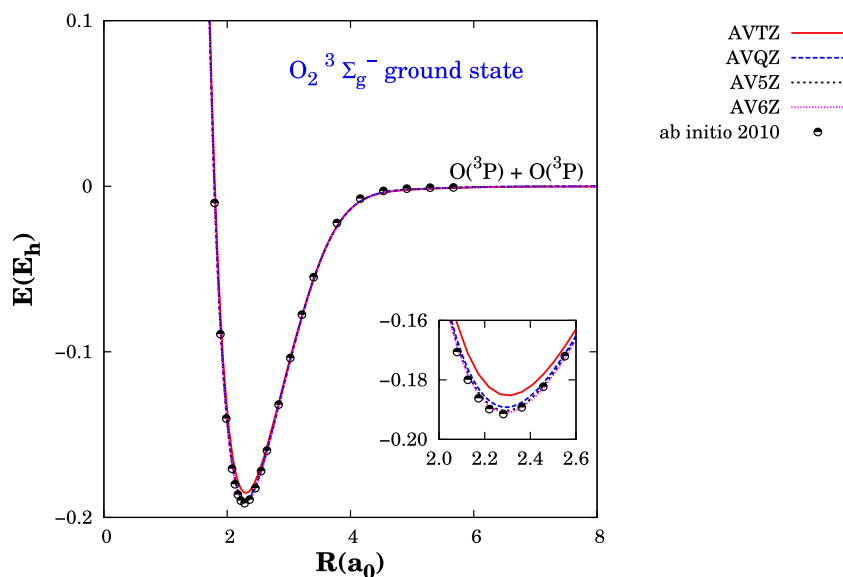
Fig. 4 Potential energy curves for the ground electronic state of the O_2 molecule calculated with different basis sets. The *circles* represent *ab initio* points calculated in Ref. [44]. In addition, also plotted in the inset is a zoom of the minimum region of the curve

for $X^3\Sigma_g^-$ were calculated with the CBS limit, in addition, corrections such as the scalar relativity, spin-orbit coupling, and the core-electron correlation are included. The energies, namely, CBS+SR+SO+CV are listed in the last column of Table I from Ref. [44]. As before, our results at AVXZ (X = 5,6) basis set are in agreement with those previously reported in Ref. [44] within the range of internuclear distances considered here. When examining the inset of this same figure, we observe that there are slight differences around the minimum between AVTZ basis set and the other ones.

Finally, in Fig. 5 are represented potential energy curves for the sulfur monoxide molecule. The circles represent *ab initio* energies reported by Borin and Ornellas at internally

contracted multi-reference configuration interaction (icM-RCI) level of theory with the cc-pVQZ basis set [45]. For completeness, the solid green line illustrates the PEC for SO molecule extracted from the DMBE potential energy surface for ground state SO_2 [46, 47]. Again, the diatomic interactions are represented according to the EHFACE2U model. It can be noted that the electronic energies in function of internuclear distances listed in column 2 of Table 1 (Ref. [45]) are between our results obtained from the AV(T+d)Z (solid red line) and AV(Q+d)Z (dashed blue line) basis set (see zoom in the minimum region). There are small differences in all energies, in particular, in the energies calculated at AV(T+d)Z basis set are larger than EHFACE2U model (0.009 E_h or 0.24 eV).

Fig. 5 Potential energy curves for the ground electronic state of the SO calculated with different basis sets. The *circles* represent *ab initio* points calculated in Ref. [45]. The *solid green line* represents the analytical form (EHFACE model) obtained in Ref. [46]. In addition, also plotted in the inset is a zoom of the minimum region of the curve
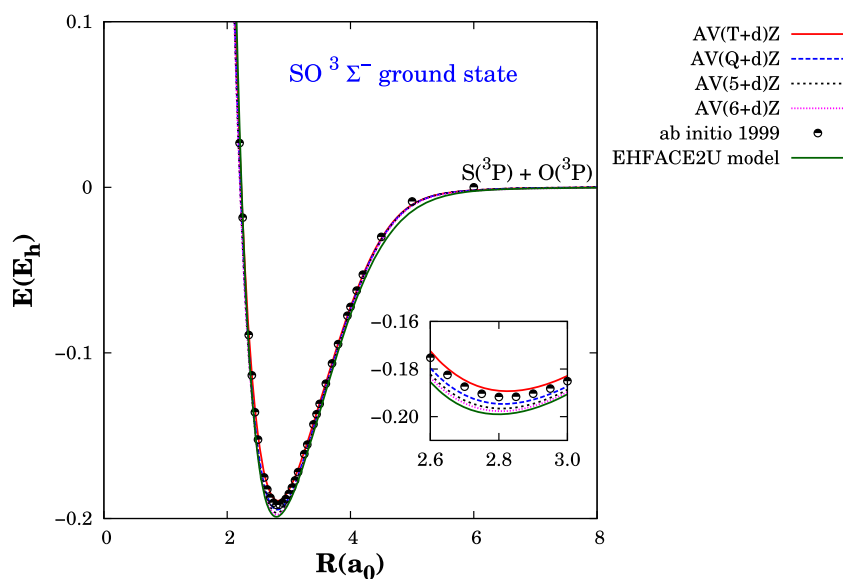
Table 1 Basis set dependence of the spectroscopic constants for the $N_2(X^1\Sigma_g^+)$

Potential	Basis set	R_e (a$_0$)	$\Delta R_e/R_e{}^a$ (%)	ω_e (cm^{-1})	$\Delta\omega_e/\omega_e{}^b$ (%)	D_e (eV)	$\Delta D_e/D_e{}^c$ (%)	$\omega_e x_e$ (cm^{-1})	$\Delta\omega_e x_e/\omega_e x_e$ (%)
Ryd.	AVTZ	2.07431	0.0	2394	1.52	9.41768	23.48	15.80	10.33
	AVQZ	2.07431	0.0	2391	1.39	9.63082	13.20	15.60	8.93
	AV5Z	2.07310	0.05	2395	1.56	9.73632	8.12	15.87	10.82
	AV6Z	2.07531	0.04	2396	1.61	9.76785	6.60	15.93	11.24
MS	AVTZ	2.06669	0.36	2449	3.85	9.54045	17.56	17.68	23.46
	AVQZ	2.08315	0.42	2399	1.73	9.76039	6.96	15.95	11.38
	AV5Z	2.05913	0.73	2474	4.91	9.88354	1.02	17.81	24.37
	AV6Z	2.05857	0.75	2476	5.00	9.91620	0.54	17.85	24.65
HH	AVTZ	2.06865	0.27	2418	2.54	9.46758	21.07	16.67	16.41
	AVQZ	2.06580	0.40	2434	3.22	9.61217	14.10	17.04	18.99
	AV5Z	2.06075	0.65	2443	3.60	9.81957	4.10	17.52	22.34
	AV6Z	2.06031	0.67	2445	3.68	9.86220	2.05	17.63	23.11
AP	AVTZ	2.09175	0.84	2326	1.35	9.44831	22.00	15.21	6.21
	AVQZ	2.08314	0.42	2349	0.38	9.69849	9.94	14.46	0.97
	AV5Z	2.08333	0.43	2345	0.55	9.77486	6.26	14.53	1.46
	AV6Z	2.08285	0.41	2346	0.50	9.80564	4.78	14.58	1.81

[a] The experimental values of ΔR_e can be seen in Table 4

[b] The experimental values of $\Delta\omega_e$ can be seen in Table 4

[c] The experimental values of ΔD_e can be seen in Table 4

Table 2 Basis set dependence of the spectroscopic constants for the $O_2(X^3\Sigma_g^-)$

Potential	Basis set	R_e (a$_0$)	$\Delta R_e/R_e{}^a$ (%)	ω_e (cm^{-1})	$\Delta\omega_e/\omega_e{}^b$ (%)	D_e (eV)	$\Delta D_e/D_e{}^c$ (%)	$\omega_e x_e$ (cm^{-1})	$\Delta\omega_e x_e/\omega_e x_e$ (%)
Ryd.	AVTZ	2.28969	0.42	1605	1.58	5.00247	8.55	13.21	10.26
	AVQZ	2.28970	0.42	1600	1.26	5.08499	4.93	13.18	10.01
	AV5Z	2.28970	0.42	1600	1.26	5.11076	3.80	13.17	9.93
	AV6Z	2.28970	0.42	1600	1.26	5.12831	3.03	13.15	9.76
MS	AVTZ	2.28889	0.39	1664	5.31	5.15345	1.93	13.72	14.52
	AVQZ	2.28115	0.05	1677	6.13	5.25710	2.61	13.78	15.02
	AV5Z	2.26425	0.69	1680	6.32	5.28918	4.02	13.82	15.35
	AV6Z	2.27939	0.02	1682	6.45	5.31066	4.96	13.85	15.60
HH	AVTZ	2.27876	0.05	1651	4.49	4.99806	8.74	13.64	13.85
	AVQZ	2.27106	0.39	1667	5.50	5.10291	4.14	13.70	14.35
	AV5Z	2.26937	0.46	1671	5.75	5.13348	2.80	13.72	14.52
	AV6Z	2.26898	0.48	1672	5.82	5.16390	1.47	13.77	14.94
AP	AVTZ	2.30267	0.99	1543	2.28	5.04119	6.85	12.80	6.84
	AVQZ	2.29298	0.56	1567	0.81	5.14910	2.12	12.45	3.92
	AV5Z	2.29152	0.50	1569	0.64	5.17947	0.79	12.39	3.42
	AV6Z	2.29166	0.51	1565	0.88	5.19745	0.001	12.42	3.67

[a] The experimental values of ΔR_e can be seen in Table 5

[b] The experimental values of $\Delta\omega_e$ can be seen in Table 5

[c] The experimental values of ΔD_e can be seen in Table 5

Table 3 Basis set dependence of the spectroscopic constants for the $SO(X^3\Sigma^-)$

Potential	Basis set	R_e (a$_0$)	$\Delta R_e/R_e{}^a$ (%)	ω_e (cm^{-1})	$\Delta\omega_e/\omega_e{}^b$ (%)	D_e (eV)	$\Delta D_e/D_e{}^b$ (%)	$\omega_e x_e$ (cm^{-1})	$\Delta\omega_e x_e/\omega_e x_e$ (%)
Ryd	AV(T+d)Z	2.79884	3.21(-4)	1204	4.87	5.17952	8.91	6.71	9.64
	AV(Q+d)Z	2.79884	3.21(-4)	1195	4.09	5.29416	4.81	6.68	9.15
	AV(5+d)Z	2.79884	3.21(-4)	1192	3.83	5.33319	3.42	6.66	8.82
	AV(6+d)Z	2.79884	3.21(-4)	1191	3.74	5.36028	2.45	6.63	8.33
MS	AV(T+d)Z	2.81980	0.74	1195	4.09	5.24626	6.52	6.68	9.15
	AV(Q+d)Z	2.81239	0.48	1211	5.48	5.40960	0.69	6.65	8.66
	AV(5+d)Z	2.80792	0.32	1216	5.92	5.46320	1.22	6.67	8.98
	AV(6+d)Z	2.80625	0.26	1218	6.09	5.49369	2.31	6.70	9.47
HH	AV(T+d)Z	2.82807	1.04	1103	3.91	4.66886	27.15	7.15	16.83
	AV(Q+d)Z	2.79948	0.02	1204	4.87	5.36251	2.37	6.40	4.57
	AV(5+d)Z	2.81032	0.41	1128	1.74	4.94807	17.18	6.73	9.96
	AV(6+d)Z	2.77639	0.80	1244	8.36	5.23775	6.83	7.05	15.19
AP	AV(T+d)Z	2.82532	0.94	1124	2.09	5.15158	9.91	6.41	4.73
	AV(Q+d)Z	2.81270	0.49	1134	1.21	5.29857	4.65	6.32	3.26
	AV(5+d)Z	2.80765	0.31	1139	0.78	5.35029	2.81	6.25	2.12
	AV(6+d)Z	2.80572	0.24	1141	0.60	5.38058	1.72	6.20	1.30

[a] The experimental values of ΔR_e can be seen in Table 6

[c] The experimental values of $\Delta\omega_e$ can be seen in Table 6.

[d] The experimental values of ΔD_e can be seen in Table 6

Spectroscopic parameters

Based on PECs obtained by fit *ab initio* points, we computed the ground state spectroscopic parameters of the molecules analyzed here determined from the Eqs. 3, 6, 24 and 43. These results are presented in the Tables 1, 2 and 3 and can be seen graphically in the Figs. 6 to 8. The column one of all tables indicates the analytical form used in the fit, whereas the basis sets are given in column two. The third, fifth, and seventh columns of these tables show calculated values of the equilibrium bond distances R_e, harmonic vibrational frequencies ω_e, and the potential well depth D_e. The relative differences between the available experimental data and the

results obtained by us given by $\Delta Y/Y$ (Y = R_e, ω_e, and D_e), are displayed in the fourth, sixth, and eighth columns, and are expressed in percentages. The experimental values adopted in this work were obtained from Refs. [48] for N_2 and [49] for O_2 and SO molecules. For completeness, the anharmonicity parameter ($\omega_e x_e$) from our curves and its comparison with the corresponding experimental values ($\Delta\omega_e x_e$) are also shown in last columns.

Although higher values of RMSD are found for the functional forms of RYD, MS, and HH, it can be seen from these tables that in general, some spectroscopic parameters obtained by these analytical representations appear to be close to the experimental results. Note that in Figs. 6, 7,
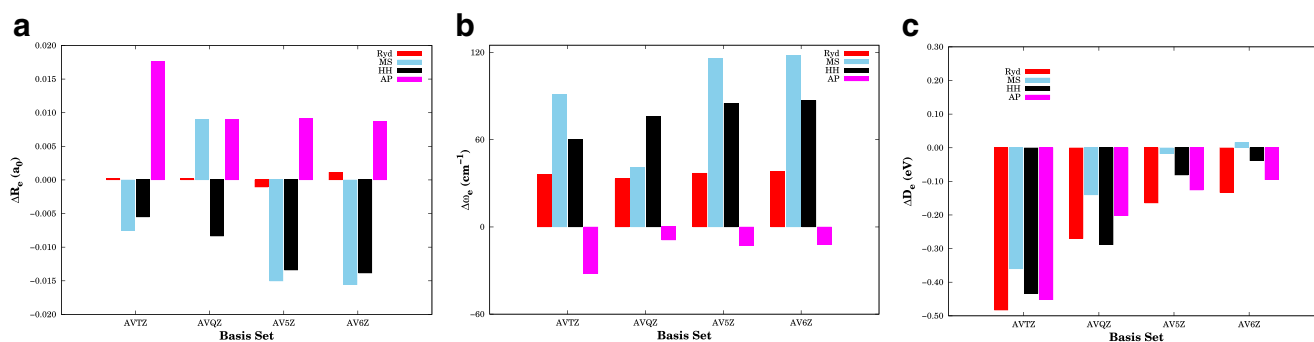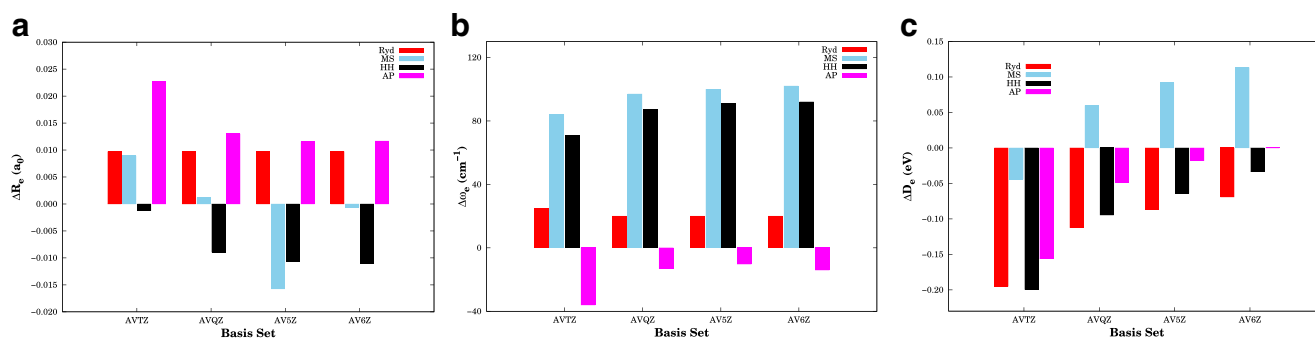
Fig. 6 Largest basis set used versus differences between our results obtained with the setup of Table 1 and the experimental data: **a** ΔR_e, **b** $\Delta\omega_e$, **c** ΔD_e for N_2 molecule. The experimental values of 2.0743 a$_0$, 2358 cm^{-1}, and 9.9008 eV are from Ref. [48]

Fig. 7 Largest basis set used versus differences between our results obtained with the setup of Table 2 and the experimental data: **a** ΔR_e, **b** $\Delta \omega_e$, **c** ΔD_e for O_2 molecule. The experimental values of 2.280 a_0, 1580 cm^{-1}, and 5.197 eV are from Ref. [49]

and 8, the red bars represent the Rydberg function, while in blue it refers to the Murrell–Sorbie potential. The black and magenta bars are used to refer to the potential HH and AP, respectively.

Notice now the results of the Table 1. Note that when we compare the bond lengths calculated by us (third column) with experimental values [48] for ground state N_2 molecule, we obtained very good agreement with relative differences of $0 \leq \Delta R_e/R_e \leq 0.84$, in percentages. Surprisingly, the results for the Rydberg function (the earliest studied here) presents almost negligible ΔR_e since their root-mean-square deviation results overestimate the threshold of chemical accuracy by about 1.2 kcal/mol. Analyzing the fourth column, the consistently increasing quality with increasing base set size only for the potential AP is remarkable. However, the results of other functions exhibit inverse behavior, i.e., increasing the size of the basis set produces bond lengths less precise. This is the case, for example, of the MS function where we obtained $DeltaR_e/R_e$ equal to 0.36% for AVTZ, 0.42% for AVQZ, 0.73% for AV5Z, and 0.75% for AV6Z. In contrast, the AP functions provide the following values for this relation: 0.84% for AVTZ, 0.42% for AVQZ, 0.43% for AV5Z and 0.41% for AV6Z. The Hulburt-Hirschfelder potential yields close

values with experimental differences of: AVTZ $\sim$ 0.007 a_0, AVQZ $\sim$ 0.008 a_0, AV5Z $\sim$ 0.001 a_0, and AV6Z $\sim$ 0.001 a_0. Such information can be seen of form summarized in Fig. 6a.

In the sixth column of the Table 1, note that the vibrational frequencies present relative differences, with $\Delta \omega_e/\omega_e$ between 0.38 and 5.0%. Comparing the values obtained for ω_e for the four potentials in question, we conclude that the best result is obtained when the functional form proposed by Aguado and Paniagua is used at MRCI(Q)/AVXZ (X = T,Q,5,6) level of theory (see also Fig. 6b). For this particular potential, our theoretical harmonic vibrational frequencies differ by less than 1.4% of the experimental values from Ref. [48]. Concerning the Rydberg function, similar results emerges from our analysis (around 1.6%), with deviations close to 38 cm^{-1} (in red), while for the MS potential are overestimated in $\sim$ 118 cm^{-1}. In addition, with respect to cardinal number X of the basis set, we obtained the values 2418, 2434, 2443, and 2445 cm^{-1}, corresponding to HH potential. In Fig. 6b, we identify that $\Delta \omega_e$ for these values (in black) slightly increases with the basis set as well as for Murrell–Sorbie potential (in blue), except in the case of aug-cc-pVQZ basis.
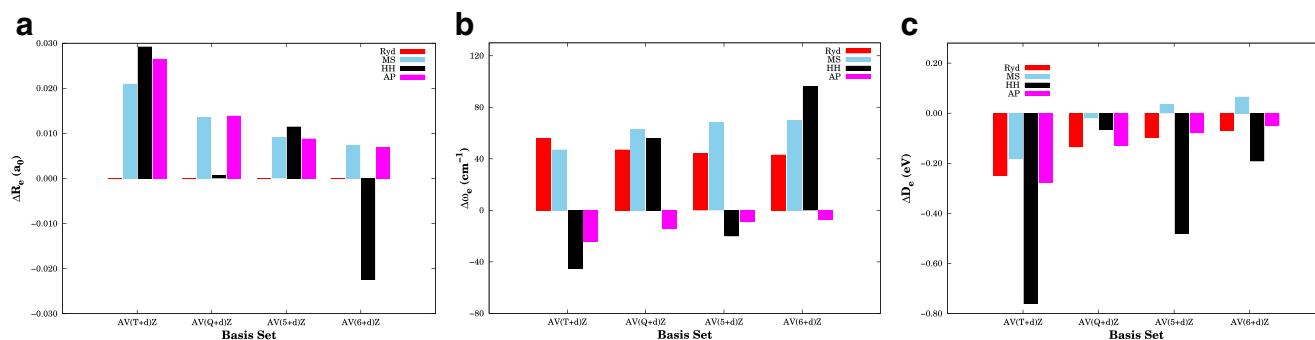

Fig. 8 Largest basis set used versus differences between our results obtained with the setup of Table 3 and the experimental data: **a** ΔR_e, **b** $\Delta \omega_e$, **c** ΔD_e for SO molecule. The experimental values of 2.7986 a_0, 1148 cm^{-1}, and 5.429 eV are from Ref. [49]

Table 4 Spectroscopic parameter from available results for $N_2(X^1\Sigma_g^+)$ molecule

Method	R_e (a_0)	ω_e (cm^{-1})	D_e (eV)	Source
NOF-OIMP2/VTZ	2.0749	–	10.004	[51]
RHF	2.0862	2971	–	[52]
CCSD(T)/V6Z	2.0732	2370	–	[53]
RMR CCSD(T)/VQZ	2.0813	2343	9.893	[54]
Exp.	2.0743	2358	9.9008	[48]

Further, in Table 1, the dissociation energies (D_e), obtained using all potentials are unexpectedly larger than the corresponding experimental values, relative differences are between 0.54 to 23.48%. This large error can be partly attributed to the fit process, in particular for AVTZ basis. Energetically, the MS potential seems to represents reasonably well the experimental value of 9.9008 eV [48], however it may differ quantitatively in more than 7% when Dunning's augmented correlation consistent valence triple-ζ basis set (aug-cc-pVTZ) is used (see Fig. 6c). From Fig. 2, one can see that the Murrell–Sorbie function has a larger depth in the well than the other functions described. This fact indicates consistency in our results. Moreover, according to Ref. [50] the reliable description of the dissociation profile of the ground state of the nitrogen molecule is a difficult problem for any *ab initio* method due to the presence of strong dynamical and nondynamical correlation effects.

Besides this study, a series of theoretical spectroscopic investigations have been performed about the N_2 system [51–54]. For the convenience of comparison, all these results are described in Table 4. In these investigations, probably the first calculations for this system, made by Fraga and Ransil [52], were made through the Hartree–Fock (RHF) restricted method. Their R_e and ω_e values are larger than the experimental results [48] by $0.01a_0$ and 613 cm^{-1}, respectively. Pawlowski et al. [53] computed the values of molecular properties by using the MP2/CCSD(T) level of theory in combination with a series of correlation-consistent basis sets. From what we know, the depth of the well was not calculated in their work. The bond length and harmonic frequency values calculated at CCSD(T)/V6Z differ of ours results with the AP function/AV6Z (and experimental) in ~ 0.009 $(0.001)a_0$ and 24 (12) cm^{-1}. Subsequently, the treatments of the nitrogen molecule using the RMR CCSD and RMR CCSD(T) methods was verified by Li and Paldus [54]. As a result, in both cases, the spectroscopic constants perform well when compared to the experimental ones. More recently, Piris, using the formulation of the natural-orbital-functional second-order-Møller-Plesset (NOF-MP2)

calculated binding energies and bond lengths for this system and others [51]. In general, the present spectroscopic parameters for the ground state of N_2 are in good agreement with the experimental [48] and previous theoretical data [51, 54].

Now, a complete discussion about the results from Table 2 and Fig. 7 for oxygen molecule is done. When equilibrium bond distances (R_e) are analyzed, the best value found corresponds to the relative difference of 0.02% for MS potential at MRCI(Q)/AV6Z level. In Fig. 7a, the Rydberg potential (in red) displays values almost constants around $0.01a_0$. On the other hand, the Table 2 shows that the deviations are in the range $0\% \leq \Delta R_e/R_e \leq 1.0\%$, which is in general agreement with Ref. [49]. An unusually large error in the AP representation leads to bond lengths with slightly overestimated (AVTZ basis), and they are more accurately predicted with the aug-cc-pV6Z basis. As one can see from Fig. 7a or in the Table 2, Rydberg and HH predictions do not improve when larger basis are used for the bond lengths. However, the O2 bond lengths are very good with the AVXZ (X = Q, 6) basis sets, with small relative errors.

The relative errors in harmonic vibrational frequencies (ω_e) are represented in Fig. 7a. The MS function predictions show a typical error of 80 to 100 cm^{-1} overestimate in most cases, whereas the AP frequencies are considerably improved, with most errors less than or equal to 1%. Obviously, the value 1569 cm^{-1} based on AV5Z is the best compared to the experimental value [49] of 1580 cm^{-1}. There is no significant deviation in this case. The values of ω_e for the Hulburt–Hirschfelder representation deviate from the experiment results by 4.49, 5.50, 5.75, and 5.82%, respectively, for the basis AVXZ (X = T, Q, 5, 6). As before, the Rydberg interaction potential (in red) shows almost constant values for vibrational frequency (near 1600 cm^{-1}). Note that this same behavior was observed in Fig. 6b. From the information contained in this figure and that displayed in Table 2 (sixth column), we can easily find that the big errors of harmonic frequencies are obtained between the functional forms of MS (blue) and HH (black).

From the energetic point of view, we found the following results:

(i) relative differences of $0.01 \leq \Delta D_e/D_e \leq 8.0$, in percentage, were calculated being the depth of the well major described when the AP function in aug-cc-pV6Z basis set is used (5.19745 eV);

(ii) as well as for N_2, here the spectroscopic constant D_e tends to smaller differences from the experimental values at MRCI level of theory with Davidson correction if we increase cardinal numbers (X = T, Q,5, and 6) of basis, however, MS (blue) does not exhibit this behavior see Fig. 7c;

Table 5 Spectroscopic parameter from available results for $O_2(X^3\Sigma_g^-)$ molecule

Method	R_e (a_0)	ω_e (cm^{-1})	D_e (eV)	Source
B3P86/CC-PV5Z	2.2676	1645	5.22	[55]
DFT/ET-QZ3P-3Diffuse	2.2733	1621	–	[56]
CI	2.3054	1614	4.72	[57]
DFT/B3LYP	2.2790	1585	5.96	[58]
MRCI(Q)	2.2979	1522	5.09	[58]
CASPT2	2.2884	1536	5.17	[58]
Exp.	2.280	1580	5.19	[49]

Table 6 Spectroscopic parameter from available results for $SO(X^3\Sigma^-)$ molecule

Method	R_e (a_0)	ω_e (cm^{-1})	D_e (eV)	Source
icMRCI/VQZ	2.8213	1137	-	[45]
icMRCI(Q)/AV5Z	2.8090	1149	5.418	[62]
CI	2.8326	1200	-	[63]
DFT/B3LYP	2.8194	1129	5.72	[58]
MRCI(Q)	2.8289	1130	5.32	[58]
CASPT2	2.8043	1125	5.40	[58]
Exp.	2.7986	1148	5.429	[49]

(iii) our results with Rydberg are underestimated by 8.55, 4.93, 3.80, and 3.03% compared to experimental values [49]. On the other hand, the AVXZ (X = Q, 5, 6) basis set for MS are overestimated by 2.61, 4.02, and 4.96%. It can be clearly seen in Fig. 2 that the well for MS is deeper than Ryd potential.

For completeness, available theoretical results from the literature are summarized in Table 5. We are also including the experimental ones from Ref. [49]. Guan et al. calculate using time-dependent density functional theory (TDDFT) with Tamm–Dancoff approximation (TDA) spectroscopic properties and potential energy curves for the six lowest bound electronic states of the oxygen molecule. In Table 5, it can be seen that their theoretical values for the ground state at this level of theory provides: Re near to experimental one and ω_e it is overestimated by $\sim$41 cm^{-1} [56]. Our values, using the AP function and AV5Z basis set, are of 1569 cm^{-1} for the harmonic frequency and 2.2915a_0 for the equilibrium bond distance, which compares better to the experimental results, particularly ω_e. Dong-Lan et al. [55] proposed a potential energy surface for SO_2 in the ground electronic state using the many-body expansion theory. Table 2 and 3, from Ref. [55] contain features such as R_e, ω_e, and D_e removed of two-body terms not only for O_2 but also for SO molecule. There, the diatomics (O_2 and SO) are modeled by the MS potential function (24) minus a extra term (c_6/R^6). As a result, the vibrational frequency is larger than the experimental one in at least 65 cm^{-1} and the depth of the well and equilibrium internuclear distance are in good agreement with your respective experimental values. However, the reported values of Schaefer obviously deviate from Ref. [49], see Table 5 for details. Finally, comparing some of our results with those of Azizi et al. [58] slight differences are found. According to them, calculations at second-order multiconfigurational perturbation theory (CASPT2) and MRCI(Q) are of comparable accuracy for few-electron systems.

For the sulfur monoxide in the ground electronic state, the spectroscopic features of the functional forms used to fitting *ab initio* points of this molecule are displayed in Table 3 and Fig. 8. The triplet state considered here converge to the dissociation limit $S(^3P) + O(^3P)$. Looking at basis set effects, all binding energies calculated are lower than the experimental one. In opposition to this, the Murrell–Sorbie energies at AV5Z and AV6Z are above by $\sim$ 0.03 and 0.06 eV, respectively. These values are close to D_e (5.429 eV) reported in Ref. [49], however, the harmonic frequencies tend to increase in approximately 40 cm^{-1}. Again, the best results observed in Table 6 are for the Aguado and Paniagua function in combination with AV(6+d)Z basis (R_e = 2.8057 a_0, ω_e = 1141 cm^{-1}, and D_e = 5.3805 eV). The same tendency holds when analyzing nitrogen and oxygen molecules (Tables 1 and 2). As can be seen from Table 3, the equilibrium bond lengths obtained for Rydberg functions reproduce the experimental value. On the other hand, this fact does not reflect better results of the other molecular features. For example, according to the present table, the frequencies for different basis sets are 1204, 1195, 1192, and 1191 cm^{-1}.

It is interesting to note that in Fig. 8a, b, and c, the Hulburt–Hirschfelder representation shows higher deviation percentages in almost all spectroscopic constants chosen, see also Table 3 for complementary information. So, one verified that for our purpose, this function is inefficient compared to the other ones. We infer that this fact can be directly connected with the values found in Fig. 1c. In general, the bond lengths and harmonic frequencies estimates for the AP function are acceptable (less than 2.1%). The main variations are predicted in the binding energy: 9.91, 4.65, 2.81, and 1.72%, respectively, for AV(T+d)Z, AV(Q+d)Z, AV(5+d)Z, and AV(6+d)Z.

Over the years, SO molecule has largely attracted interest due to its high reactivity. Furthermore, sulfur monoxide has been detected in interstellar clouds and in the atmospheres of planets [59]. Its interest goes beyond the astrophysical studies being necessary in areas such as combustion

[60] and photodissociation [61]. From extensive literature, the spectroscopic properties of both experimental and theoretical were chosen from Refs. [45, 58, 62, 63] in order to compare our results. These values are conveniently listed in Table 6. As discussed, Borin and Ornellas calculated *ab initio* PECs at icMRCI/VQZ level of theory with the intention of studying the singlet and triplet states of sulfur monoxide. As a result, deviations from the experimental values for ground state (triplet state) were obtained by differences of $0.0227a_0$ for bond length and 11 cm^{-1} for vibrational frequency. These data show smaller variations of our best results: $0.0156a_0$ and 4 cm^{-1}. Unfortunately, an important constant, D_e, was not evaluated. In 2011, Yu and Bian performed the icMRCI calculations in combination with the aug-cc-pV5Z basis sets. The R_e, ω_e, and D_e values they provide for the SO($X^3\Sigma^-$) are $2.8090a_0$, 1149 cm^{-1}, and 5.418 eV, respectively. It is observed good accord between the present spectroscopic parameters and our results, and consequently, with experimental ones. Data reported in Ref. [63] are also collected in Table 6. In such a work, a complete study for seven low-lying electronic states of sulfur monoxide is reported by Swope et al., carried out using configuration interaction (CI). They were found that ω_e it is overestimated around 52 cm^{-1}. Again, D_e was also not evaluated for this work. All other results in Table 6 refer to Ref. [58] except the last line (Exp.) that contain values from Ref. [49]. It is interesting to note that all harmonic vibrational frequencies in Table 6 are smaller than the corresponding experimental value to 1148 cm^{-1} [49]. On the contrary, reported values for Re are larger than the corresponding experimental measurement.

In general, the spectroscopic constants here predicted are in excellent agreement with previous theoretical and experimental results. Therefore, we can conclude that the AP function obtained at MRCI(Q)/ aug-cc-pV6Z level of theory can well describe the interaction potential of the sulfur monoxide molecule in the ground state. Furthermore, the same functional form presents similar results for other molecules investigated by us.

Conclusions

In the present paper, *ab initio* calculations at MRCI with Davidson corrections have been performed followed by aug-cc-pvXZ (X = T, Q, 5, 6) basis set. The PECs obtained are fitted in order to compute the molecular features of the spectroscopic region. Test calculations were made for the following benchmark model potentials in selected systems such as N_2, O_2 and SO, all in their respective ground electronic states. Analyzing the six potentials described

here, we are concerned with several aspects: the number of parameters, easy to obtain the potential energy curves and their quality in the short and long-range regions. Furthermore, we are also interested in the diversity of diatomic systems where each potential can be applied.

The potential of Hulburt–Hirschfelder was highlighted by being represented by a function involving five relatively simple parameters to be manipulated. The fact that it contained more parameters, thus ensuring greater flexibility, was also a defining point. However, due to a signal error kept during a certain period, its function was considered unsatisfactory. Once corrected, the HH potential was considered, in most cases, one of the best with five parameters for fitting particularly the asymptotic region, where the Morse curve was not so properly behaved [17]. It should also be noted that the Aguado and Paniagua method promotes a much quicker calculation of the self-consistency tests of the eigenvalues of the Schrödinger radial wave equation, i.e., of the energies that are essential for the construction of the potential energy surface [1].

Although the study of analytical forms to describe potential energy surfaces for diatomic systems has been explored for more than a century (the first records date back to 1874 [64]), we believe this issue is not fully depleted. Even with formulations like Xie and Hsu's [65], with a universal functional form, applied to 200 diatomic systems, many other proposals are still emerging (see for example Zhang et al. [66], Yu and Zhiwei [67] with further universal propositions, Yu [68], Bouazis [69]). In addition, as Hooydok pointed out, the Xie and Hsu model did not appear universal, as initially claimed by the authors [70]. For example, such a model is not applicable in common bonds with elements of the VII group and inaccurately reproduce the H_2 prototype [70]. There is a crucial point that led us to conduct this analysis with some rather old representations. By fitting the potentials and their respective spectroscopic constants with the computational methodologies today available, we have obtained more precise data than those reported in the past. This is especially notable in relation to those that precede MBE. Such precision for the diatomic systems chosen in this particular study was what most interested us. We believe the accuracy of an analytic or numerical functional form describing a PEC is at least as important as obtaining an universal representation.

References

1. Aguado A, Camacho JJ, Paniagua M (1992) A numerical procedure to obtain accurate potential energy curves for diatomic molecules. J Mol Struc (THEOCHEM) 254:135–144. https://doi.org/10.1016/0166-1280(92)80059-U

2. Visser R, Van Dishoeck EF, Black JH (2009) The photodissociation and chemistry of CO isotopologues: applications to interstellar clouds and circumstellar disks. Astron Astrophys 503:323–343. https://doi.org/10.1051/0004-6361/200912129

3. Crispim LWS, Hallak PH, Benilov MS, Ballester MY (2018) Modelling spark-plug discharge in dry air, Combust . Flame 198:81–88. https://doi.org/10.1016/j.combustflame.2018.09.007

4. Ballester MY, Varandas AJC (2007) Theoretical study of the reaction $OH + SO \rightarrow H + SO_2$. Chem Phys Lett 433:279–285. https://doi.org/10.1016/j.cplett.2006.11.074

5. Bell MT, Softley TM (2009) Ultracold molecules and ultracold chemistry. Mol Phys 107:99–132. https://doi.org/10.1080/00268970902724955

6. Zanchet A, Roncero o González-LezanaT, Rodríguez-López A, Aguado A, Sanz-Sanz C, Gómez-Carrasco S (2009) Differential cross sections and product rotational polarization in a+ BC reactions using wave packet methods: $h^+ + d_2$ and $Li + HF$ examples. J Phys Chem A 113(52):14488–14501. https://doi.org/10.1021/jp9038946

7. Marx D, Hutter J (2009) Ab initio molecular dynamics: Basic theory and advanced methods 11-22. Cambridge University Press, New York

8. Morais VMF (1990) Estudos Teóricos sobre Superfícies de Energia Potencial e Dinâmica Molecular em Trímeros de Metais Alcalinos. Dissertação (Doutorado em Química)- Instituto de Ciências Biomédicas Abel Salaza, Universidade do Porto, Porto. Cambridge University Press, New York

9. Rydberg R (1931) Graphische Darstellung einiger Bandenspe-ktroskopischer Ergebnisse [J]. Z Phys 73:376–385. https://doi.org/10.1007/BF01341146

10. Morse PM (1929) Diatomic molecules according to the wave mechanics. II. Vibrational levels. Phys Rev 34:57–64. https://doi.org/10.1103/PhysRev.34.57

11. Varshni YP (1957) Comparative study of potential energy functions for diatomic molecules. Rev Mod Phys 29:664–682. https://doi.org/10.1103/RevModPhys.29.664

12. Hulburt HM, Hirschfelder JO (1941) The energy levels of a rotating vibrator. J Chem Phys 9:61–69. https://doi.org/10.1063/1.1750827

13. Dunham JL (1932) The energy levels of a rotating vibrator. Phys Rev 41:721–731. https://doi.org/10.1103/PhysRev.41.721

14. Hulburt HM, Hirschfelder JO (1961) Erratum: Potential energy functions for diatomic molecules. J Chem Phys 35:1901–1902. https://doi.org/10.1063/1.1732171

15. Tawde NR, Gopalakrishnan K (1954) Hulbert-hirschfelder U(r) function in C2(Swan) system. Ind J Phys 28:469-472. ISSN: 0019–5480

16. Herzberg G (1950) Spectra of diatomic molecules d. Van Nostrand Company, New Jersey

17. Tawde NR, Katti MR (1962) Comments on "Potential energy function for diatomic molecules". J Chem Phys 37:674–675. https://doi.org/10.1063/1.1701396

18. Murrell JN, Sorbie KS (1974) New analytic form for the potential energy curves of stable diatomic states. J Chem Soc Faraday Trans 2(70):1552–1556. https://doi.org/10.1039/F29747001552

19. Klein OZ (1932) Zur Berechnung von Potentialkurven für zweiatomige Moleküle mit Hilfe von Spektraltermen. Z Phys 76:226–235. https://doi.org/10.1007/BF01341814

20. Rees ALG (1947) The calculation of potential-energy curves from band-spectroscopic data. Proc Phys Soc Lond 59:998–1008. https://doi.org/10.1088/0959-5309/59/6/310

21. Thakkar AJ (1975) A new generalized expansion for the potential energy curves of diatomic molecules. J Chem Phys 602:1693–1701. https://doi.org/10.1063/1.430693

22. Simons G, Parr RG, Filan JM (1973) A new alternative to the Dunham potential for diatomic molecules. J Mol Struct 59:3229–3234. https://doi.org/10.1063/1.1680464

23. Lennard-Jones JE (1924) On the determination of molecular fields: II: from the equation of state of a gas. Proc R Soc Lond A 106(738):463–477. https://doi.org/10.1098/rspa.1924.0082

24. Hua W (1990) Four-parameter exactly solvable potential for diatomic molecules. Phys Rev A 42:2524–2529. https://doi.org/10.1103/PhysRevA.42.2524

25. Levine IN (1966) Accurate potential-energy function for diatomic molecules. J Chem Phys 45:827–828. https://doi.org/10.1063/1.1727689

26. Aguado A, Paniagua M (1992) A new functional form to obtain analytical potentials of triatomic molecules. J Chem Phys 96(2):1265–1275. https://doi.org/10.1063/1.462163

27. Murrell JN, Carter S, Farantos SC, Huxley P, Varandas AJC (1984) Molecular potential energy functions. Wiley, New York

28. Aguado A, Tablero C, Paniagua M (1998) Global fit of ab initio potential energy surfaces I. Triatomic systems. Comput Phys Commun 108:259–266. https://doi.org/10.1016/S0010-4655(97)00135-5

29. Lulu Z, Song Y-Z, Gao S, Ji-Hua X, Yong Z, Meng Q (2016) Accurate theoretical study on the ground and first-excited states of Na2: potential energy curves, spectroscopic parameters, and vibrational energy levels. Can J Phys 94(12):1–20. https://doi.org/10.1139/cjp-2016-0438

30. Werner H-J, Knowles PJ (1985) A second order multiconfiguration SCF procedure with optimum convergence. J Chem Phys 82:5053–5063. https://doi.org/10.1063/1.448627

31. Werner H-J, Knowles PJ (1988) An efficient internally contracted multiconfiguration-reference configuration interaction method. J Chem Phys 89:5803–5814. https://doi.org/10.1063/1.455556

32. Wan MJ, Huang DH, Fan QC, Jiang G (2013) A study of the low-lying states at multi-reference configuration interaction level of N2 molecule. Indian J Phys 87:245–250. https://doi.org/10.1007/s12648-012-0217-9

33. Streit L, Machado FBC, Custodio R (2011) Double ionization energies of HCl, HBr, cl_2 and br_2 molecules: An MRCI study. Chem Phys Lett 506:22–25. https://doi.org/10.1016/j.cplett.2011.02.047

34. Hochlaf M, Ndome H, Hammoutène D, Vervloet M (2010) Valence–Rydberg electronic states of n_2: Spectroscopy and spin–orbit couplings. J Phys B 43(1-7):245101. https://doi.org/10.1088/0953-4075/43/24/245101

35. Dunning Jr. TH, Peterson KA, Wilson AK (2001) Gaussian basis sets for use in correlated molecular calculations. X. The atoms aluminium through argon revisited. J. Chem. Phys. 114:9244–9253. https://doi.org/10.1063/1.1367373

36. Werner H-J, Knowles PJ, Knizia G, Manby FcR, Schütz M, Celani P, Korona T, Lindh R, Mitrushenkov A, Rauhut G et al (2010) MOLPRO, version 2010.1, a package of ab initio programs. See http://www.molpro.net

37. Silva ML, Guerra V, Loureiro J, Sá PA (2008) Vibrational distributions in n_2 with an improved calculation of energy levels using the RKR method. Chem Phys 348:187–194. https://doi.org/10.1016/j.chemphys.2008.02.048

38. Politzer P, Toro-Labbé A, Gutiérrez-Oliva S, Murraya JS (2012) Perspectives on the reaction force. Book: Adv Quantum

Chem 64:189–209. https://doi.org/10.1016/B978-0-12-396498-4.00006-5

39. Zhang L-L, Song Y-Z, Gao S-B, Xu J-H, Zhou Y, Meng Q-T (2016) Accurate theoretical study on the ground and first-excited states of na_2: potential energy curves, spectroscopic parameters, and vibrational energy levels. Can J Phys 94:1259–1264. https://doi.org/10.1139/cjp-2016-0438

40. Mills K, Spanner M, Tamblyn I (2017) Deep learning and the Schrödinger equation. Phys Rev A 96(1-9):042113. https://doi.org/10.1103/PhysRevA.96.042113

41. Xiao-Niu Z, De-Heng S, Jin-Feng S, Zun-Lue Z (2010) Elastic scattering of two ground-state N atoms. Chin Phys B 19(1-8):013501. https://doi.org/10.1088/1674-1056/19/1/013501

42. Poveda LA, Varandas AJC (2003) Accurate single-valued double many-body expansion potential energy surface for ground-state HN_2. J Phys Chem A 107:7923–7930. https://doi.org/10.1021/jp030571o

43. Varandas AJC, Silva JD (1992) Potential model for diatomic molecules including the united-atom limit and its use in a multiproperty fit for argon. J Chem Soc Faraday Trans 88:941–954. https://doi.org/10.1039/FT9928800941

44. Bytautas L, Matsunaga N, Ruedenberg K (2010) Accurate ab initio potential energy curve of o_2. II. Core-valence correlations, relativistic contributions, and vibration-rotation spectrum. J Chem Phys 132(1-15):074307. https://doi.org/10.1063/1.3298376

45. Borin AC, Ornellas FR (1999) The lowest triplet and singlet electronic states of the molecule SO. Chem Phys 247:351–364. https://doi.org/10.1016/S0301-0104(99)00229-3

46. Rodrigues SPJ, Sabín JA, Varandas AJC (2002) Single-valued double many-body expansion potential energy surface of ground-state SO_2. J Phys Chem A 106:556–562. https://doi.org/10.1021/jp013482p

47. Varandas AJC, Rodrigues SPJ (2002) A realistic double many-body expansion potential energy surface for $SO_2(x^1a')$ from a multiproperty fit to accurate ab initio energies and vibrational levels. Spectrochim Acta A 58:629–647. https://doi.org/10.1016/S1386-1425(01)00661-8

48. Le Roy RJ, Huang Y, Jary C (2006) An accurate analytic potential function for ground-state n_2 from a direct-potential-fit analysis of spectroscopic data. J Chem Phys 125(1-12):164310. https://doi.org/10.1063/1.2354502

49. Huber KP, Herzberg G (1979) Molecular Spectra and Molecular Structure, Vol. IV Constants of diatomic molecules. Van Nostrand Reinhold, New York

50. Chattopadhyay S, Chaudhuri RK, Mahapatra US (2008) Application of improved virtual orbital based multireference methods to n_2, LiF, and c_4h_6 systems. J Chem Phys 129:244108. https://doi.org/10.1063/1.3046454

51. Piris M (2018) Dynamic electron-correlation energy in the natural-orbital-functional second-order-Møller-Plesset method from the orbital-invariant perturbation theory. Phys Rev. A 98(1-6):022504. https://doi.org/10.1103/PhysRevA.98.022504

52. Fraga S, Ransil BJ (1961) Studies in molecular structure. V. Computed spectroscopic constants for selected diatomic molecules of the first row. J Chem Phys 35:669–678. https://doi.org/10.1063/1.1731987

53. Pawlowski F, Halkier A (2003) Jørgensen P Accuracy of spectroscopic constants of diatomic molecules from ab initio calculations. J Chem Phys 118:2539–2549. https://doi.org/10.1063/1.1533032

54. Li X, Paldus J (2008) Full potential energy curve for n_2 by the reduced multireference coupled-cluster method. J Chem Phys 129:054104. https://doi.org/10.1063/1.2961033

55. Dong-Lan W, An-Dong X, Xiao-Guang Y, Hui-Jun W (2012) The analytical potential energy function of flue gas $SO_2(x^1a_1)$. Chin Phys B 21(1-6):043103. https://doi.org/10.1088/1674-1056/21/4/043103

56. Guan J, Wang F, Ziegler T, Cox H (2006) Time-dependent density functional study of the electronic potential energy curves and excitation spectrum of the oxygen molecule. J Chem Phys 125(1-9):044314. https://doi.org/10.1063/1.2217733

57. Schaefer III HF (1971) Ab initio potential curve for the $x^3\Sigma_-$ state of o_2. J Chem Phys 54:2207–2211. https://doi.org/10.1063/1.1675154

58. Azizi Z, Roos BO, Veryazov V (2006) How accurate is the CASPT2 method? Phys Chem Chem Phys 8:2727–2732. https://doi.org/10.1039/B603046G

59. Lam C-S, Wang H, Xu Y, Lau K-C, Ng CY (2011) A vacuum-ultraviolet laser pulsed field ionization-photoelectron study of sulfur monoxide (SO) and its cation (SO^+). J Chem Phys 134(1-7):144304. https://doi.org/10.1063/1.3575227

60. Glarborg P, Kubel D, Dam-Johansen K, Chiang H-M, Bozzelli JW (1996) Impact of SO_2 and NO on CO oxidation under post-flame conditions. Int J Chem Kinet 28:773–790. https://doi.org/10.1002/(SICI)1097-4601(1996)28:10<773::AID-KIN8>3.0.CO;2-K

61. Chen X, Asmar F, Wang H, Weiner BR (1991) Nascent sulfur monoxide (x3. SIGMA.-) vibrational distributions from the photodissociation of sulfur dioxide, sulfonyl chloride, and dimethylsulfoxide at 193 nm. J Phys Chem 95:6415–6417. https://doi.org/10.1021/j100170a007

62. Le Y, Bian W (2011) Extensive theoretical study on electronically excited states and predissociation mechanisms of sulfur monoxide including spin–orbit coupling. J Comput Chem 32:1577–1588. https://doi.org/10.1002/jcc.21737

63. Swope WC, Lee Y-P, Schaefer III HF (1979) Sulfur oxide: low-lying bound molecular electronic states of SO. J Chem Phys 71:3761–3769. https://doi.org/10.1063/1.438783

64. Roscoe HE, Schuster A (1874) I. Note on the absorption-spectra of potassium and sodium at low temperatures, Proc. Roy Soc Lond 22:362–365. https://doi.org/10.1098/rspl.1873.0062

65. Xie RH, Hsu PS (2006) Universal reduced potential function for diatomic systems. Phys Rev Lett 96(1-4):243201. https://doi.org/10.1103/PhysRevLett.96.243201

66. Zhang GD, Liu JY, Zhang LH, Zhou W, Jia CS (2012) Modified Rosen-Morse potential-energy model for diatomic molecules. Phys Rev A 86(1-5):062510. https://doi.org/10.1103/PhysRevA.86.062510

67. Yu CF, Zhiwei W (2011) A universal analytic potential function applied to diatomic molecules. IEEE 3rd Int. Conf. Commun. Soft. Net:105–110. https://doi.org/10.1109/ICCSN.2011.6014229

68. Yu CF (2015) A novel high-precision analytic potential function for diatomic molecules. Key Eng Mater 645:313–318. https://doi.org/10.4028/www.scientific.net/KEM.645-646.313

69. Bouaziz D (2015) Kratzer's molecular potential in quantum mechanics with a generalized uncertainty principle. Ann Phys 355:269–281. https://doi.org/10.1016/j.aop.2015.01.032

70. Hooydonk GV (2008) Comment on "Universal Reduced Potential Function for Diatomic Systems". Phys Rev Lett 100(1):159301. https://doi.org/10.1103/PhysRevLett.100.159301